Magnetic Resonant Coupling Wireless Power Transfer for Light-Weight Batteryless UAVs

Alessandro Torrisi and Davide Brunelli
DII, University of Trento, Italy
{alessandro.torrisi, davide.brunelli}@unitn.it

***Abstract*—This paper presents a concrete solution for flying a lightweight drone completely without batteries. The drone can float upon a transmitting coil indefinitely and prevents from battery lifetime limitations, by exploiting a magnetic resonant coupling for wireless power transfer. We used a DC-DC converter to match the load impedance at the WPT. Finally, the overall achieved maximum efficiency is 40% measured over different distances.**

***Index Terms*—magnetic resonant coupling, wireless power transfer, DC-DC converter, UAVs, drone, batteryless**

I. Introduction

Nowadays, drones and unmanned aerial vehicles (UAVs) are gaining momentum and often utilized for several outdoor and indoor applications. The most common scenarios are related to hazardous environment monitoring and mapping. A more challenging application uses UAVs as carriers for item transportation. For such applications, the UAV usually follows a repetitive flight path, and small-sized drones are preferred for indoor missions. Nevertheless, the weight and size constraints cause strict battery lifetime limitations, and short-lasting missions can be planned before battery replacement or recharging. In this paper, we present a wireless power transfer system designed to work around the limited onboard energy of UAVs.

Wireless power transfer (WPT) through the use of magnetic resonant coupling is a well known and growing technology for all portable devices, and several wireless systems are already available on the market. They are usually implemented as a battery charger for mobile phones, vehicles, and UAVs [1]. In industrial applications [2], wireless power transfer technology is used where a wired connection or a battery pack could be a limitation in the operations. WPT is an attractive way to power devices without a cable connection and has found application even in the biomedical field [3].

This paper contributes to investigating the possibility of flying a battery-less drone with WPT. The aim is to let the drone fly in a mid-air range of 30-40cm indefinitely. As a proof of concept, a magnetic resonant coupling WPT is used with a resonance frequency above 400kHz. A detailed simulation is performed to show and analyze the behavior of a resonant magnetic coupling WPT system, to reveal the strong dependencies on the load resistance. Measurements are carried out to validate the simulation results.

Finally, the setup is built, the receiving coil is mounted on a Crazyflie 2.0 drone without its battery. An AC-DC interface with a buck converter is used to couple the receiving coil to the drone's electronic circuitry. Since the battery has been completely removed from the drone, we achieved roughly the same gravimetric density.

Thank to the WPT, the battery lifetime has been extended indefinitely. Moreover, if the weight is reduced, we also achieved an increase in the payload capacity. However, a significant reduction in the operating area is introduced. To enhance the operating area, a set of different coils or a 3D coil [4] can be used, which will be a task for future work.

The rest of the article is organized as follows. Section II introduces the related works, and Section III introduces to the design of the WPT Magnetic Resonant Coupling. Section IV presents the efficency and charaterizaiton of the system. Section V concludes the paper with final remarks.

II. Related Work

Wireless power transfer and drones have already captured the interest of researchers, with particular attention to the battery charging without a wired connection [5]. Two well-defined standards are available for charging mobile devices, the Qi standard developed by the Wireless Power Consortium, and the WiPower standard provided by the Alliance For Wireless Power. The standards define not only the power transfer model, but also the methods to control the power flow from the transmitter to the receiver, exploiting a feedback signal on the same wireless link.

This work aims to transfer enough power to remove the battery completely and get the drone flying at a reasonable distance range. Khan et al. [6] proposed to transfer power over long distance (about 0.5m) to charge and power mobile devices in an indoor environment. They used an extremely large pair of coils, preventing the system to be embedded in a real mobile device. Likewise, Han et al. [4] used a 3D transmitter coil with a 3D intermediate coil for a quasi-omnidirectional coverage.

In this work, we use a two-coil setup in a real scenario with a real drone floating in the mid-air range upon the transmitting coil. The power consumption on the receiving side is not constant due to the necessary adjustment of the throttle to stabilize the drone. Moreover, the drone requires a specific supply voltage. A DC-DC converter is used to adjust the output voltage at the receiving coil. This aspect is crucial, introducing a non-constant variation in the equivalent load impedance at the WPT system output. The variation changes the power efficiency over the distance. Indeed, the resonant magnetic coupling WPT system behavior is strongly related to the load

resistance. By exploiting this phenomenon, a larger distance coverage is achieved.

III. Basics on Magnetic Resonant Coupling WPT

Magnetic resonant coupling WPT is a widely used technology that exploits two tuned coils (primary and secondary coils) operating at the same resonant frequency. Different topologies are available to tune the two coils. In this work, we utilize the series-series compensation schematic (Fig. 1). The choice on the compensation is related to the values of tank capacitors, that are not affected by load changes, and the rectifier circuit, which does not require an inductor (i.e., heavy components on board of the drone). As Jaros at el. [7] proposed for medium range and low power transfer application.

A brief analysis of the circuit can be done by assuming the overall system frequency response with a high-quality factor at the resonance (namely resonance frequency $\tilde{\omega}_o$) and a low-pass filter behavior for higher frequencies. It permits to consider the circuit operating with sinusoidal waves, at least nearby the resonance frequency. In this way, the square wave generated by the inverter is then considered only with its fundamental harmonic at frequency ω_o. Likewise, the rectifier circuit with the real load (smoothing capacitor and load resistance) can be represented equivalently to a secondary-side resistance R_{eq}. Indeed, all the higher harmonics are neglected. In figure Fig. 2 the equivalent model is depicted and simplified.

As discussed, the rectifier, the filter capacitor and the load can be considered as an equivalent resistance $R_{eq} = 8/\pi^2 R_l$, neglecting the voltage drop of the diode bridge and referring to figure Fig. 1 for the evaluation of R_l. Moreover, the presence of the DC-DC converter introduces another coefficient m on the equivalent load resistance. Neglecting the power loss due to the DC-DC converter, the equivalent load resistance is evaluated in the equation (2):

$$R_l = \frac{V_{dc}}{I_{dc}} \simeq \frac{V_{dc}^2}{V_{load}^2} R_{load} = \frac{R_{load}}{m^2} \tag{1}$$

$$R_{eq} = \frac{8}{\pi^2} R_l \simeq \frac{8}{\pi^2} \frac{R_{load}}{m^2} \tag{2}$$

The model in figure Fig. 2 can be simplified and easily described using Kirchfoff voltage law at the primary and secondary side (3) to obtain the output power as a function of the mutual inductance M. By assuming the resonance frequency equal for both sides, the output power is simplified in (5), where the reactive components are neglected because their reactance cancels out.

$$\begin{cases} V_{in} = I_p(Z_p + Z_{ref}) \\ j\omega M(d) I_p = I_s(Z_s + R_{eq}) \end{cases} \tag{3}$$

Where:

$$\begin{aligned} Z_s &= R_s + j\omega L_s + \tfrac{1}{j\omega C_s} \\ Z_p &= R_p + j\omega L_p + \tfrac{1}{j\omega C_p} \\ Z_{ref} &= -\tfrac{j\omega M I_s}{I_p} = \tfrac{\omega^2 M^2}{Z_s + R_{eq}} \end{aligned}$$

$$P_{out} = |I_s|^2 R_{eq} = \frac{\omega^2 M^2 V_{in}^2 R_{eq}}{|Z_p(Z_s + R_{eq}) + \omega^2 M^2|^2} \tag{4}$$

$$P_{out} = \frac{\omega^2 M^2 V_{in}^2 R_{eq}}{[R_p(R_s + R_{eq}) + \omega^2 M^2]^2} \tag{5}$$

The mutual inductance M is the coefficient depicting how the coils are coupled, i.e., the geometrical arrangement of the windings where the main factor is the distance d between the two coils. It plays the primary role in the wireless power transfer.

As a first approach, the mutual inductance is evaluated in formula (6) referring to circular coils where r_p, r_s are the coil radius and N_p, N_s are the coil turn number. It is used for early assessment of WPT performance over the distance between the coils.

$$M(d) = \frac{\pi \mu_0 N_p N_s (r_p r_s)^2}{2d^3} \tag{6}$$

A. Simulations

We carried out some simulations using MatLab. By exploiting formulas (4 and 6), the model is simulated with different equivalent load resistance R_{eq}. The output power is given by sweeping the distance (and so the M) between primary and secondary coils. The parameters used for the simulation, listed in table I, refer to the real implemented scenario. The two coils are tuned about $f_{res} = 379kHz$.

Considering a $V_{sup} = 1V$ and the inverter as an ideal configuration of two switches in a single leg, the V_{in} is evaluated as follows:

$$V_{in} = \frac{4}{\pi} \frac{V_{sup}}{2} = \frac{4}{\pi} \frac{1}{2} = 0.63[V] \tag{7}$$

The simulation result, shown in Fig. 3, reveals the maximum output power as a function of the distance, the peak power position strongly depends on the equivalent load resistance. The peak amplitude is strongly dependent also on the overall stray resistance of the circuit. It is useful in combination with a DC-DC converter. Indeed, the variation on the equivalent load resistance can be exploited to maximize the power transfer efficiency over a wider distance between the coils. For instance, by reducing the R_{eq}, the peak power is moved toward a longer distance. Vice-versa, if the R_{eq} is increased, the peak power moves towards a reduced range.

TABLE I
List of the WPT system parameters

Primary parameters		Secondary parameters	
L_p	$198[\mu H]$	L_s	$18.7[\mu H]$
N_p	14	N_s	10
r_p	$195[mm]$	r_s	$45[mm]$
C_p	$884[pF]$	C_s	$9.1[nF]$
R_p	$0.70[\Omega]$	R_s	$0.67[\Omega]$

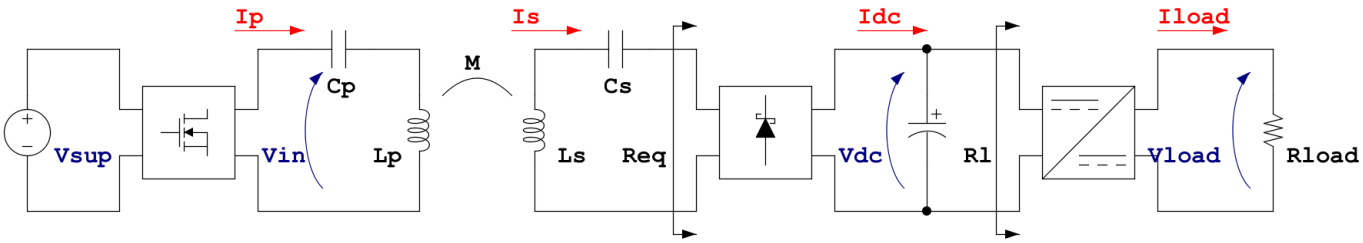

Fig. 1. Overall WPT system block diagram with the series-series compensation topology and the DC-DC converter

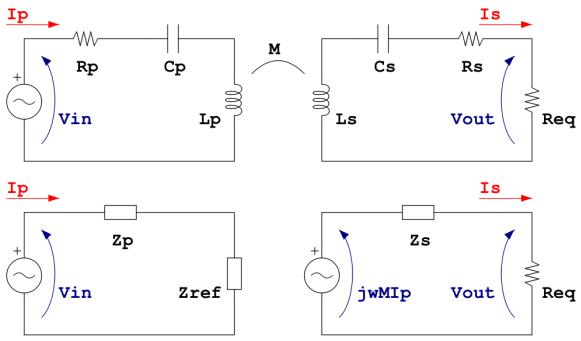

Fig. 2. Simplification of the resonant magnetic coupling WPT schematization

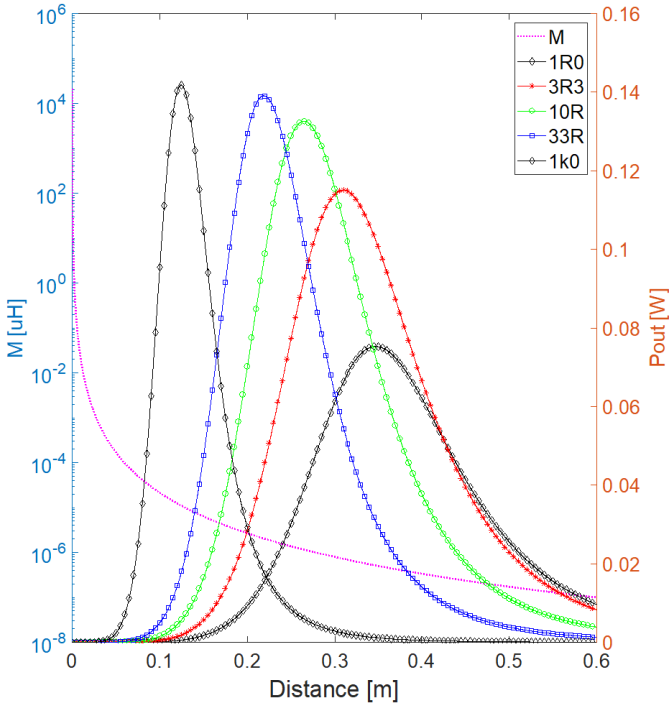

Fig. 3. Simulation of the WPT power output over the distance in combination with different equivalent load resistance R_{eq}. Resonance frequency evaluated about 379kHz.

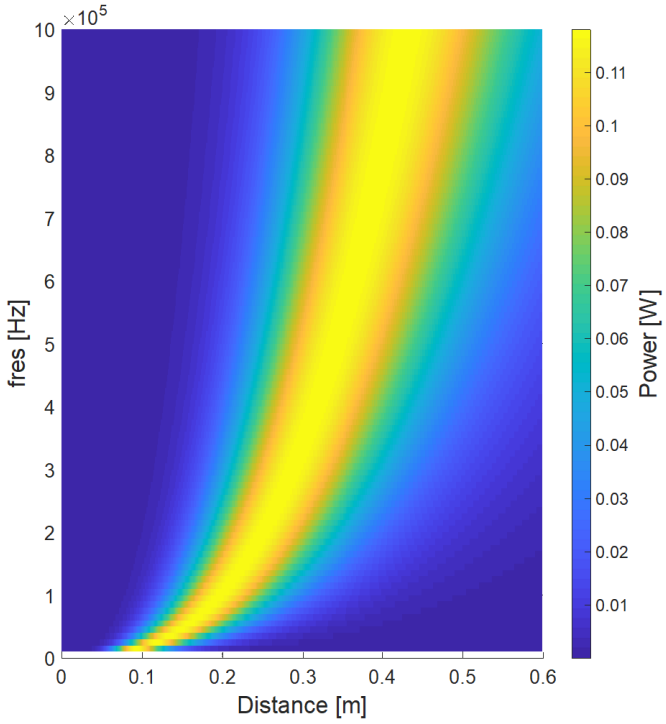

Fig. 4. Simulation of the WPT output over the distance and the resonance frequency with a fixed equivalent load resistance $R_{eq} = 3.3\Omega$.

A second simulation, with the same parameters (i.e., the same coils configuration table I), is conducted assuming the same resonance frequency for primary and secondary coils and using (5). The simulation shows a sweep over the resonance frequency for a fixed equivalent load resistance $R_e = 3.3\Omega$. The value has been used because it is close to the one that the drone exhibits during normal operations. This simulation assumes that all the reactive components cancels out, and the stray resistance does not change over the frequency. Even though it is a strong assumption because the parasitic resistance of the coils slightly increases at higher frequencies, we did not measure a significant impact on the output power. The simulation also shows a clear relationship between distances and resonance frequency.

Moreover, the simulation in figure Fig. 4 reveals that the out-

put peak power remains all most constant over the frequency and suggests that design tradeoffs are required. For instance, if a frequency of 500kHz is considered as a starting point, a 1MHz resonance frequency does not double the distance for the peak power. Moreover, a higher resonance frequency could involve substantial parasitic effects, like skin effect on the coil conductors. The cost also increases, because high-frequency inverters need more complex circuits and more expensive components. A good tradeoff is a resonance frequency of 400kHz.

These simulations are useful to understand the behavior of the magnetic resonant coupling WPT to achieve the best results in terms of transferred power and distances.

B. Circuit Description

The system is developed, using the block diagram in figure Fig. 1. The invert has been designed as a single leg single-ended output that drives the primary side. Low R_{dsON} fast switching power MOSFET IRFP4668 are used as switching elements. The inverter output is a square wave with a fixed frequency and amplitude manually set using a variable power supply and an arbitrary function generator.

For this experiment, a pair of coils are designed and compensated. The parameter of the coils are listed in table I. The proposed secondary side is based on a Schottky diode full-bridge rectifier and a capacitive filter. A DC-DC buck converter is exploited to supply the drone properly. The primary role of the buck converter is to operate a resistance matching between the drone and the output of the rectifier, referring to figure Fig. 1 R_l and R_{load}. The output voltage is set on roughly $V_{load} = 4V$. The LMZ36002 integrated circuit is used as an integrated power supply module for DC/DC conversion. It has an integrated power inductor, and it is suitable for a wide input voltage range. The overall efficiency of the module, including the bridge rectifier, has been measured in the range 81-94 % according to the input and the load condition.

IV. Results

The preliminary measurements aim at validating the model and the simulations. The setup is built and measurements are done with a fixed equivalent load resistance $R_{eq} = 3.3\Omega$ (referring to the block diagram in Fig. 1). In figure Fig. 5 the result is shown where the real behavior (blue curve) is pretty close to the simulated one (red curve).

It is important to notice that the simulation is adjusted with a lower input voltage $V_{in} = 0.54V$ to match the real value measured at the output of the inverter stage. This scaling is to take into account the relatively large dropout of the inverter stage. Anyway, the curves are the same in comparison with the first simulation (Fig. 3), as confirmed in figure Fig. 6. The remaining slight difference between the two curves is due to non-ideality in the coupling, the coils' arrangement, and other parasitic aspects, like stray inductances in the connection.

After that, the fixed equivalent load resistor is changed with the rectifier, the DC-DC buck converter, and a fixed output load resistance of $R_{load} = 2\Omega$. The measurement is repeated

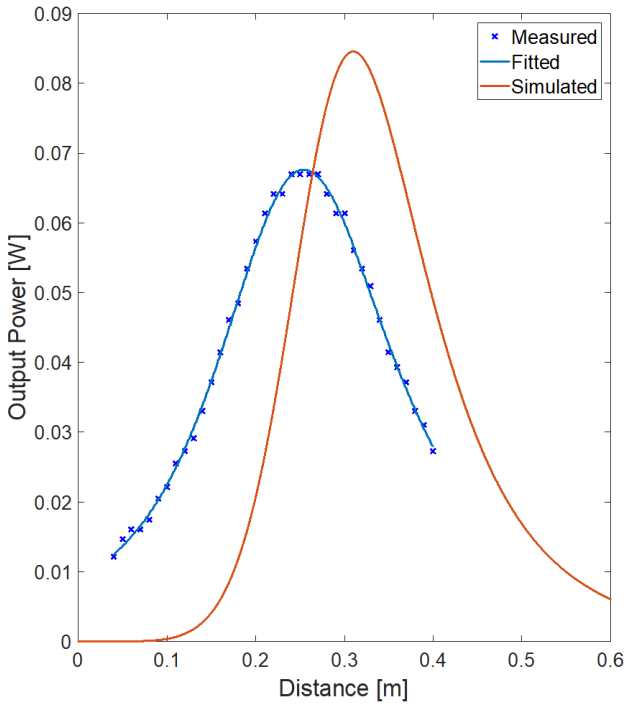

Fig. 5. Comparison on the received power measurement on the implemented WPT system with a fixed equivalent load resistance $R_{eq} = 3.3\Omega$ and the simulated one with a $V_{in} = 0.54V$.

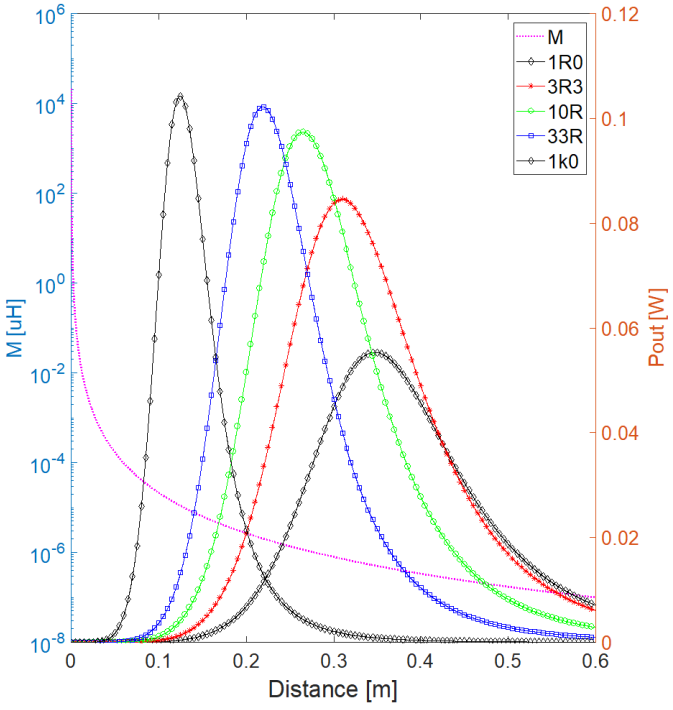

Fig. 6. Simulation of the WPT power output over the distance in combination with different equivalent load resistance R_{eq}. Resonance frequency evaluated about 379kHz and $V_{in} = 0.54V$.

with a 12 bits oscilloscope and V_{sup}, I_{sup}, V_{dc} and I_{dc} are measured.

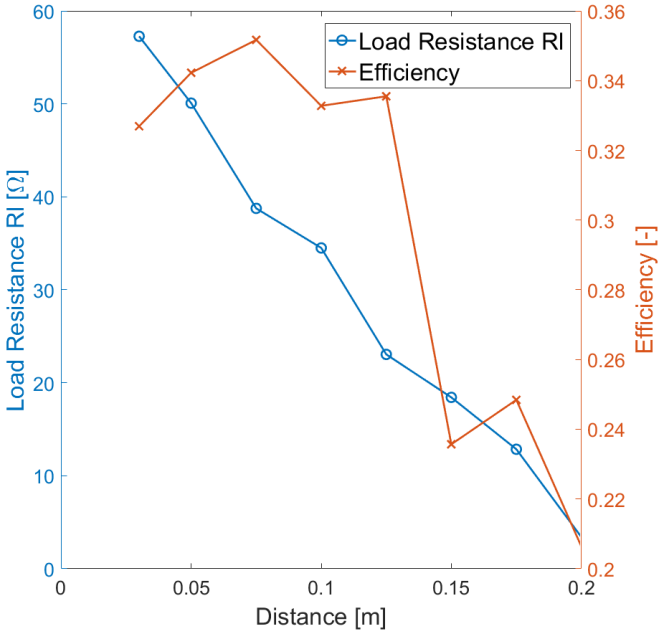

Fig. 7. Overall WPT efficiency and load resistance R_l on a fixed output power of about 8W ($R_{load} = 2\Omega$ e $V_{load} \simeq 4V$).

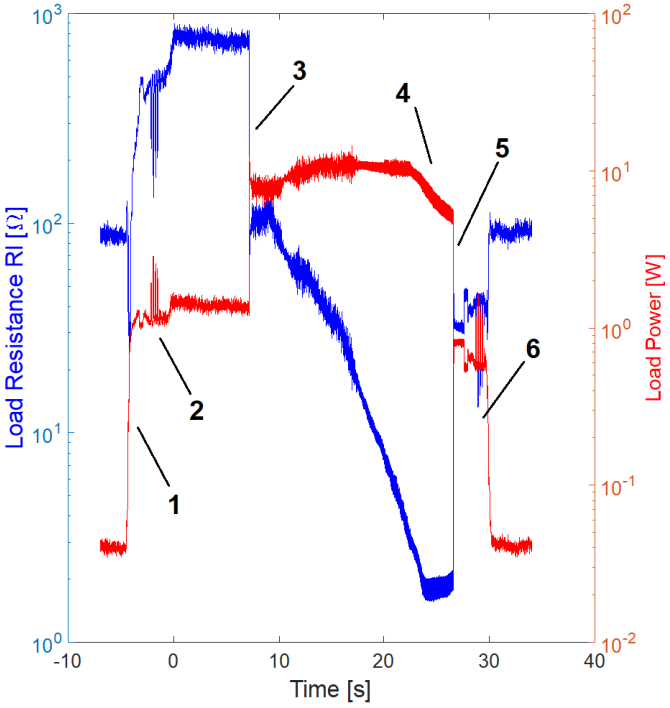

Fig. 8. Output power and load resistance R_l on the flying drone. From the start-up (1) and initialization of the engines (2), full throttle (3), power drop due to overcoming on the covered distance for the WPT (4), shut down (5) and finally re-initialization (6).

The overall WPT system efficiency, evaluated from the input power given by the source and the load, is calculated in the following formula (referring to the block diagram in Fig. 1):

$$\eta_{tot} = \frac{V_{sup} I_{sup}}{V_{dc} I_{dc}} \tag{8}$$

$$R_l = \frac{V_{dc}}{I_{dc}} \tag{9}$$

$$P_l = V_{dc} I_{dc} \tag{10}$$

This includes the efficiency of the magnetic resonant WPT, the inverter stage power loss, the rectifier power loss, and all the other parasitic phenomena. However, the DC-DC converter is not taken into account.

In figure Fig. 7

Finally, the fixed load resistor is changed with the drone, and the measurement is repeated. Differences in the same measurements depend on the moving parts of the drone. Thus V_{sup} is adjusted to transfer enough power for a full-throttle of the drone's motor. Instead of a static measurement with fixed positions, a movement is done along the direction from the transmitting coil. A sweep over the distance is carried out maintaining the same throttle, in figure Fig. 8 it can be seen that the power consumption is almost constant.

In Fig. 8, the drone power consumption P_l and the load resistance R_l are depicted. They are calculated with formulas (9) and (10). As the distance increases, the load resistance decreases due to the automatic adjustment of the DC-DC buck converter. The measurements are done until the distance is too high, and the power transferred is not enough for throttle and drone hovering.

In Fig. 9, the measurement results reveal the overall efficiency of the system during the drone's flight about 35%, a good result considering the range of covered distances. However, the higher the distance between the drone and the transmitting coil, the lower the voltage; thus the resistance is low due to weak coupling. This phenomenon is derived by the presence of the DC-DC buck converter. An interesting scenario is depicted where the efficiency of the overall system remains all most constant over the distance. It is an important consequence because the range is strongly improved, and the drone can fly at a higher distance from the transmitter without problems in the supplied power.

V. Conclusion

By exploiting wireless power transfer technologies, we demonstrated that a UAV can fly without batteries. We developed and assessed a real system, and we analyzed interesting features of the WPT. A considerable distance coverage with an excellent overall efficiency has been achieved by utilizing a DC-DC buck converter.

Future work would focus on improving the WPT setup (i.e., mini-UAV and transmitter) to enhance the covered distances.

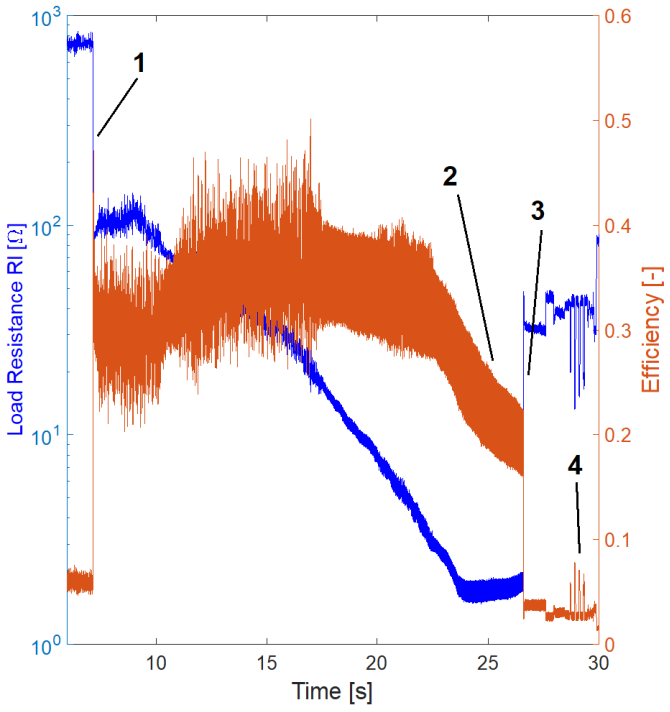

Fig. 9. Overall WPT efficiency and load resistance R_l on the flying drone. Focus on the flight from the startup of the engine (1) until the shut down (3). Evidence of the power drop due to an higher distance (2) and re-initialization of the drone (4).

Fig. 10. Photo of the tiny drone Crazyflie with the receiving coil mounted.

We plan to develop a closed-loop path with multiple wireless power transmitters to get the drone flying indefinitely and to improve the feedback control between power intake and throttle.

ACKNOWLEDGMENT

This research was supported by the IoT Rapid-Proto Labs projects, funded by Erasmus+ Knowledge Alliances program of the European Union (588386-EPP-1-2017-FI-EPPKA2-KA).

REFERENCES

[1] C. Wang and Z. Ma, "Design of wireless power transfer device for uav," in *2016 IEEE International Conference on Mechatronics and Automation*, Aug 2016, pp. 2449–2454.

[2] C. Florian, M. Grossi, K. Veliu, R. P. Paganelli, F. Berra, D. Masotti, M. Lanzoni, A. Santarelli, B. Ricc, M. Gavesi, and A. Costanzo, "A 150-w ir wpt embedded system at 6.78-mhz for the supply and control of linear motors," in *2018 IEEE Wireless Power Transfer Conference (WPTC)*, June 2018, pp. 1–4.

[3] C. Liu, C. Jiang, J. Song, and K. T. Chau, "An effective sandwiched wireless power transfer system for charging implantable cardiac pacemaker," *IEEE Transactions on Industrial Electronics*, vol. 66, no. 5, pp. 4108–4117, May 2019.

[4] W. Han, K. T. Chau, C. Jiang, W. Liu, and W. H. Lam, "Design and analysis of quasi-omnidirectional dynamic wireless power transfer for fly-and-charge," *IEEE Transactions on Magnetics*, vol. 55, no. 7, pp. 1–9, July 2019.

[5] S. Aldhaher, P. D. Mitcheson, J. M. Arteaga, G. Kkelis, and D. C. Yates, "Light-weight wireless power transfer for mid-air charging of drones," in *2017 11th European Conference on Antennas and Propagation (EUCAP)*, March 2017, pp. 336–340.

[6] I. Khan, M. I. Qureshi, M. U. Rehman, and W. T. Khan, "Long range wireless power transfer via magnetic resonance," in *2017 Progress in Electromagnetics Research Symposium - Fall (PIERS - FALL)*, Nov 2017, pp. 3079–3085.

[7] V. Jaros, P. Drgona, B. Kozacek, and M. Piri, "Analytical comparison of topology configuration of wireless power transfer system," in *2016 International Conference on Applied Electronics (AE)*, Sep. 2016, pp. 107–110.